Evolution of Enzymatic Activities in the Enolase Superfamily: Partitioning of Reactive Intermediates by (*D*)-Glucarate Dehydratase from *Pseudomonas putida*†

David R. J. Palmer,‡ Brian K. Hubbard,§ and John A. Gerlt*,‡,§

Departments of Biochemistry and Chemistry, University of Illinois at Urbana−Champaign, Urbana, Illinois 61801

Received May 14, 1998; Revised Manuscript Received August 18, 1998

ABSTRACT: Glucarate dehydratase (GlucD) from *Pseudomonas putida* catalyzes the dehydration of both (*D*)-glucarate and (*L*)-idarate to 3-deoxy-(*L*)-*threo*-2-hexulosarate as well as their epimerization. (*D*)-[6-^{13}C]Glucarate and (*L*)-[6-^{13}C]idarate have been synthesized for use in continuous assay of the reactions catalyzed by GlucD by both ^{13}C and ^{1}H NMR spectroscopies, thereby allowing the simultaneous measure of both the dehydration and epimerization reactions. Substrate and solvent isotope effects for the dehydration reactions have been quantitated. The mechanism of the GlucD-catalyzed reaction is discussed in the context of that previously established for the homologous mandelate racemase from *P. putida*, also a member of the enolase superfamily whose members catalyze reactions initiated by abstraction of a proton α to a carboxylate group.

In eubacteria, (*D*)-glucarate dehydratase (GlucD)[1] catalyzes the Mg^{2+}-dependent dehydration of (*D*)-glucarate to 3-deoxy-(*L*)-*threo*-2-hexulosarate [5-keto-4-deoxy-(*D*)-glucarate or 5-KDG; Scheme 1; ref *1*]. In Pseudomonads and *Bacillus subtilis*, 5-KDG is processed to α-ketoglutarate via the sequential action of 5-KDG dehydratase/decarboxylase and α-ketoglutarate semialdehyde dehydrogenase (upper pathway in Scheme 1; refs *2* and *3*). In *Escherichia coli* and other enterobacteria, 5-KDG is processed to pyruvate and 2-phosphoglycerate via the sequential action of 5-KDG aldolase, tartronate semialdehyde reductase, and glycerate kinase (lower pathway in Scheme 1; ref *4*).

Primary sequences are available for the GlucDs from *Pseudomonas putida*, *B. subtilis*, and *E. coli*; these are members of the enolase superfamily (*5*). All of the members of this superfamily apparently are related by their ability to catalyze reactions that are initiated by abstraction of a proton from a carbon atom adjacent to a carboxylate group. In addition to GlucD, members of this superfamily include enolase, mandelate racemase (MR), muconate lactonizing enzyme (MLE), (*D*)-galactonate dehydratase (GalD), and at least six other enzymes.[2] On the basis of the startlingly similar high-resolution crystal structures for enolase, MR, and MLE I and the alignment of the primary sequences of superfamily members, we expect that the active sites of all members of the superfamily are located in β-barrel (TIM barrel) domains. Furthermore, we expect that mechanistic insights available for characterized family members can be used in a predictive fashion to facilitate elucidation of both general and specific catalytic strategies used by all members of the superfamily.

The available structures and primary sequence alignments (*5*) indicate that a common catalytic strategy is employed by all members of the superfamily: a divalent metal ion (typically Mg^{2+}) coordinated to a conserved binding site allows Lewis acid stabilization of an enolic intermediate generated by abstraction of the α-proton. Additionally, in the mandelate racemase (MR) subgroup of the superfamily, those enzymes that can deprotonate a substrate having the (*S*)-configuration contain a KXK sequence motif in which the functional group of the second Lys acts as the (*S*)-specific base; those enzymes that can deprotonate a substrate of the (*R*)-configuration contain a His-Asp dyad in which the His acts as the (*R*)-specific base; and those enzymes that can deprotonate substrates of both the (*R*)- and (*S*)-configurations contain both sequence motifs. On the basis of the primary sequence alignments, the GlucDs are predicted to contain the necessary catalytic residues to deprotonate substrates of both (*R*)- and (*S*)-configurations.

† This research was supported by Grants GM-40570 and GM-52594 from the National Institutes of Health.

* Address correspondence to this author (e-mail: j-gerlt@uiuc.edu).

‡ Department of Biochemistry, University of Illinois.

§ Department of Chemistry, University of Illinois.

[1] Abbreviations: GlucD, (*D*)-glucarate dehydratase; 2-KDG, 3-deoxy-(*D*)-*erythro*-2-hexulosarate or 2-keto-3-deoxyglucarate; 5-KDG, 3-deoxy-(*L*)-*threo*-2-hexulosarate or 5-keto-4-deoxy-(*D*)-glucarate; MLE I, muconate lactonizing enzyme I; MR, mandelate racemase.

[2] The enzymatically characterized members of the superfamily include (*5*) enolase from a variety of organisms; mandelate racemase from *Pseudomonas putida* (MR); muconate lactonizing enzyme I (unsubstituted *cis*,*cis*-muconate as substrate) from *P. putida* and *Acinetobacter calcoaceticus*; muconate lactonizing enzyme II (halogenated *cis*,*cis*-muconate as substrate) from *P. putida*, *Alcaligenes eutrophus*, and *Pseudomonas* sp. P51; (*D*)-galactonate dehydratase (GalD) from *Escherichia coli*; (*D*)-glucarate dehydratases (GlucD) from *P. putida*, *Bacillus subtilis*, and *E. coli* (orf f446, bp 8295−9635 in GenBank Accession ECAE000362; ref *4*); β-methylaspartate ammonia lyase from *Clostridium tetanomorphum*; *o*-succinylbenzoate synthases from *Amycolatopsis* sp., *B. subtilis*, *E. coli*, *Haemophilus influenzae*, *Staphylococcus aureus*, and *Synechocystis* PCC6803; and cMyc promoter binding protein from *Homo sapiens*. The members of the superfamily catalyzing uncertain or unknown reactions include carboxyphosphenolpyruvate synthase from *Streptomyces hygroscopicus*; RspA from *E. coli*; Spa2 from *Streptomyces ambofaciens*; SpaA from *Streptomyces coelicolor*; rTS-α from *H. sapiens*; rTS-β from *H. sapiens*; orf f446 (bp 9656−10996 in GenBank Accession ECAE000362; ref *4*) from *E. coli*; and orf f405 (bp 10660−11877 in GenBank Accession ECAE000314) from *E. coli*.

S0006-2960(98)01122-2 CCC: $15.00
Published on Web 09/25/1998

Scheme 1

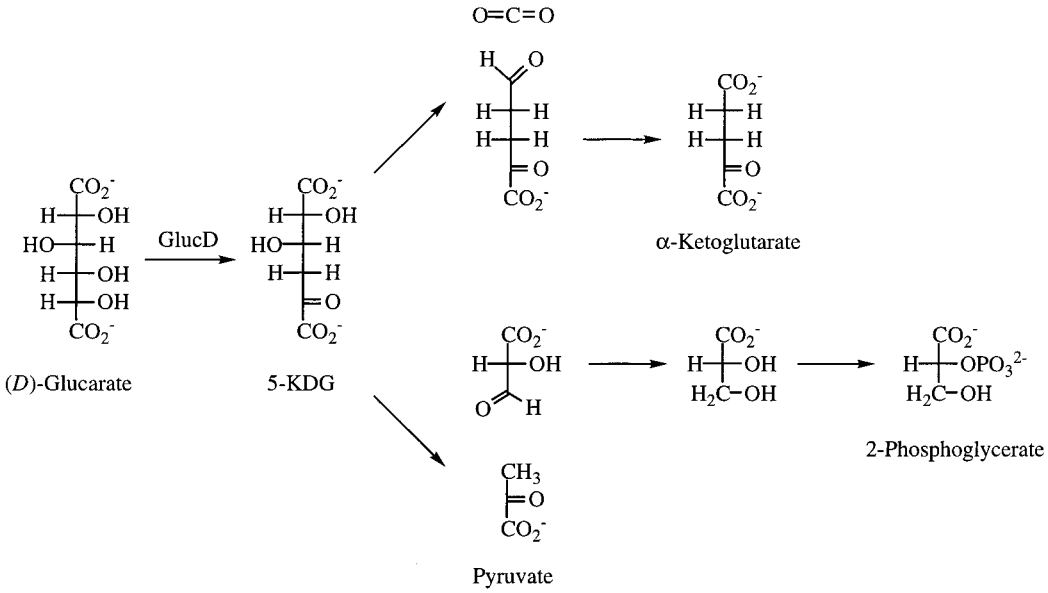

Although the reaction catalyzed by GlucD from *P. putida* was studied more than 30 years ago, the correct reaction was delineated only recently by studies reported by this laboratory using insights provided by its membership in the MR subgroup of the enolase superfamily. The GlucDs from *E. coli* (*1*) and from *P. putida* (*2*, *3*) were reported to convert (*D*)-glucarate not only to 3-deoxy-(*L*)-*threo*-2-hexulosarate [5-keto-4-deoxy-(*D*)-glucarate; 5-KDG; initiated by proton abstraction from carbon-5] but also to 3-deoxy-(*D*)-*erythro*-2-hexulosarate (2-keto-3-deoxyglucarate, 2-KDG; initiated by proton abstraction from carbon-2) in ratios of 85:15 and 92:8, respectively.

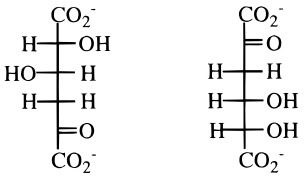

With both enzymes, the earlier interpretations were based on studies in which the fate of the label in [1-^{14}C]-(*D*)-glucarate was determined following periodate oxidation of the reaction product(s) to formylpyruvate and glyoxylate; in each case, the label was primarily found in glyoxylate, but a smaller amount was also found in formylpyruvate, suggesting dehydration to a mixture of 2-KDG and 5-KDG, in which the latter predominated.

(*D*)-Glucarate and (*L*)-idarate are epimers at carbon-5, with (*D*)-glucarate and (*L*)-idarate having 5-(*S*) and 5-(*R*) absolute configurations, respectively.

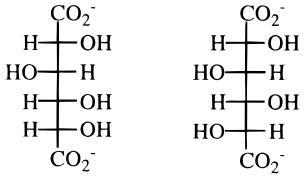

We discovered (*6*) that the results of the earlier studies had been misinterpreted as a result of the formation of (*L*)-idarate from (*D*)-glucarate during the course of the GlucD-catalyzed dehydration reaction by competing epimerization of carbon-5, as shown in Scheme 2. Because (*L*)-idarate is symmetrical, the integrity of the isotopic label in the 1-carboxylate group of (*D*)-glucarate is lost in the epimerization reaction, resulting in the formation of both 1- and 6-labeled samples of 5-KDG and not a mixture of 1-labeled samples of 5-KDG and 2-KDG, as originally reported. Using (*D*)-[1-^{13}C]glucarate, we demonstrated with ^{1}H and ^{13}C NMR spectroscopies that at the completion of the reaction only a single product is produced in which the isotopic label is distributed in a ratio of 85:15 between carbons-1 and -6 of 5-KDG. We also determined that (*L*)-idarate had a value of k_{cat} similar to that of (*D*)-glucarate but a larger K_m. Similar observations have been made in this laboratory using the GlucD from *E. coli* (*4*).

In this paper we report the use of both ^{1}H and ^{13}C NMR spectroscopies to quantitate the partitioning of the (first) enolic intermediate in Scheme 2 between dehydration and epimerization catalyzed by the GlucD from *P. putida*. Substrate and solvent deuterium kinetic isotope effects have been measured that provide insights into the energetics of formation and processing of the reaction intermediates. The results are discussed in the context of the enolase superfamily with a comparison especially to the reaction catalyzed by MR, thereby providing insights regarding the evolution of enzymatic activities in this superfamily.

In the following paper (*7*), we report a high-resolution X-ray structure for the GlucD from *P. putida* that confirms the expected structural homology with MR and supports the functional homology described in this paper. In the third paper (*4*), we report the identification and functional characterization of the enzymes in the catabolic pathway for (*D*)-glucarate and galactarate in *E. coli*.

MATERIALS AND METHODS

^{1}H and ^{13}C NMR spectra were recorded using Varian Unity Inova and Unity 500 MHz NMR spectrometers, respectively.

Scheme 2

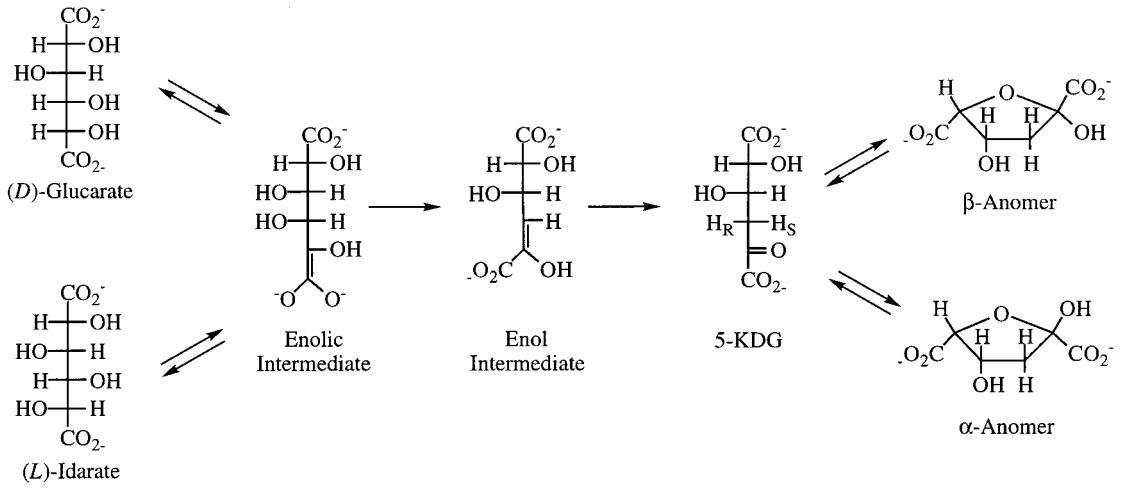

UV absorbance measurements were made with a Perkin-Elmer Lambda-14 spectrophotometer. Isotopically labeled (^{2}H and ^{13}C) reagents were obtained from Cambridge Isotopes Ltd. (*D*)-Glucarate was obtained from Aldrich. All other reagents were the highest quality grade commercially available.

Preparation of GlucD. The gene encoding GlucD from *P. putida* was cloned into the expression plasmid pET-17b using the *Nde*I and *Hin*dIII restriction sites and expressed in *E. coli* BL21(DE3) cells following induction with 0.4 mM isopropyl thiogalactoside. GlucD was purified from sonicated cells by ion-exchange chromatography using a 50 mL column of Chelating Sepharose Fast Flow in the Ni^{2+} form eluted with 10 volumes of 50 mM imidazole in 50 mM Tris-HCl, pH 7.9, followed by a 12 volume linear gradient of 50−200 mM imidazole in 50 mM Tris-HCl, pH 7.9. After dialysis against 50 mM Tris-HCl, pH 8.0, containing 10 mM $MgCl_2$, the enzyme was subjected to gel filtration using a column of Sephacryl S400 (2 × 85 cm) followed by anion-exchange chromatography using a Pharmacia Resource-Q column (6 mL) eluted with a 15 volume gradient of 0−0.2 M NaCl in 50 mM Tris-HCl, pH 8.0, containing 10 mM $MgCl_2$.

Synthesis of (*L*)*-Idarate*. (*L*)-Iditol was prepared by sodium borohydride reduction of (*L*)-sorbose (32 g, 178 mmol), recrystallization of the (*L*)-iditol product as its hexaacetyl derivative (*8*), and methanolysis with NaOMe/MeOH. (*L*)-Iditol (4.8 g, 26 mmol) was oxidized in concentrated HNO_3 according to the method of Mehltretter (*9*): 10 mL of concentrated HNO_3 to which 0.02 g of $NaNO_2$ had been added was heated to 60 °C. (*L*)-Iditol was added slowly over the course of 20 min. The mixture was stirred at 65 °C for 3 h, after which time it was cooled in an ice bath and the pH was adjusted to 11 with 45% aqueous KOH. The solution was stored at 4 °C for 16 h, filtered, and applied to an anion-exchange column (AG-1X8, formate, 3 × 66 cm). (*L*)-Idarate was eluted at 4 °C using a linear gradient of 0−2 M formic acid over 1.625 L, and the effluent was collected in 25 mL fractions. Fractions were tested for the presence of a substrate for GlucD after an aliquot was adjusted to pH 8 using 0.5 M Tris base. (*L*)-Idarate was obtained by concentration of the GlucD-reactive fractions to dryness, dissolution of the residue in a minimum volume of H_2O, titration to pH 11 with 45% KOH to ensure delactonization, careful addition of HCl to pH ∼4, and precipitation of the monopotassium salt by addition of 2-propanol. The solid was recrystallized twice from H_2O−2-propanol to yield fine white needles (0.660 g, 2.7 mmol, mp 172−173 °C): ^{1}H NMR δ (D_2O) 4.16 [s, H-2(5)], 3.92 [s, H-3(4)].

Synthesis of (*L*)-[*2,5-$^2H_2$*]*Idarate*. 5-Ketofructose was obtained from a culture of *Gluconobacter cerenius* grown for 14 days at 30 °C in 500 mL of growth medium containing 60 g of fructose, 5% peptone, and 2% yeast extract (*10*). Cells were removed by centrifugation, and the medium was decanted and decolorized with carbon. Salts were removed by stirring with Dowex mixed bead resin AG501-X8(D), H^+ and OH^- forms. The resulting solution was concentrated in vacuo and lyophilized. The remaining solid was 5-ketofructose (47 g). Reduction of the gummy solid (16 g) with sodium borodeuteride (4 g) in 250 mL of H_2O resulted in a crude mixture of [2,5-$^2H_2$]alditols, from which [2,5-$^2H_2$]iditol was isolated and converted to (*L*)-[2,5-$^2H_2$]idarate as described for the unlabeled substrate. Yield: 0.303 g; mp 171−172 °C; ^{1}H NMR δ (D_2O) 3.91 [s, H-3(4)]; ^{13}C NMR δ (D_2O) 177.0 [C-1(6)], 72.5 [C-3(4)]. A ^{1}H NMR resonance that could be associated with (*L*)-[2,5-$^1H_2$]idarate was not observed.

Synthesis of (*D*)-[*2,3,4,5-$^2H_4$*]*Glucarate*. Perdeuterated (*D*)-glucose (0.99 g, 5.3 mmol) was oxidized in concentrated HNO_3 as described above. (*D*)-[2,3,4,5-$^2H_4$]Glucarate crystallized from the reaction mixture at pH 4 as described for unlabeled (*D*)-glucarate (*8*) and was recrystallized from H_2O (0.604 g, 2.5 mmol, mp 187 °C): ^{13}C NMR δ (D_2O) 177.1 (C-1), 176.8 (C-6).

Synthesis of (*D*)-[*6-^{13}C*]*Glucarate and* (*L*)-[*1*(*6*)*-^{13}C*]*Idarate*. (*D*)-[6-^{13}C]Glucarate and (*L*)-[1(6)-^{13}C]idarate were synthesized using the Killiani−Fischer cyanohydrin strategy (*11*). Reaction of (*L*)-xylose (4.95 g, 0.033 mol) with K^{13}CN (2.25 g, 0.034 mol) yielded a mixture of (*L*)-[1-^{13}C]-idonate and (*L*)-[1-^{13}C]gulonate. The mixture was oxidized by its slow addition in a 20 mL aqueous solution to 10 mL of concentrated HNO_3 and treatment as described above for synthesis of unlabeled (*L*)-idarate. Anion-exchange chromatography resulted in partial separation of the two products. The fractions were pooled into (*D*)-glucarate- and (*L*)-idarate-containing fractions, and each was concentrated, adjusted to pH 11, and rechromatographed twice. The (*D*)-[6-^{13}C]-

Table 1: Values of Kinetic Parameters

substrate	k_{cat} (s^{-1})	K_m (10^6 M)	k_2[a] ($M^{-1}\ s^{-1}$)	KIE[b]
(*D*)-glucarate				
pH 8.0	17 ± 3	67 ± 6	2.5×10^5	$k_{cat}^{H_2O}/k_{cat}^{D_2O} = 2.1$
pD 8.0	8.0 ± 0.4	13 ± 7	6.2×10^5	$k_2^{H_2O}/k_2^{D_2O} = 0.40$
(*L*)-idarate				
pH 8.0	21 ± 4	180 ± 10	1.2×10^5	$k_{cat}^{H_2O}/k_{cat}^{D_2O} = 3.0$
pD 8.0	7.1 ± 0.5	62 ± 9	1.1×10^5	$k_2^{H_2O}/k_2^{D_2O} = 1.1$
(*D*)-glucarate-d_4				
pH 8.0	4.2 ± 0.2	86 ± 11	4.9×10^4	$k_{cat}^{H}/k_{cat}^{D} = 4.1$ $k_2^{H}/k_2^{D} = 5.1$
(*L*)-idarate-d_2				
pH 8.0	8.6 ± 0.4	92 ± 9	9.3×10^4	$k_{cat}^{H}/k_{cat}^{D} = 2.6$ $k_2^{H}/k_2^{D} = 1.3$

[a] $k_2 = k_{cat}/K_m$. [b] KIE = kinetic isotope effect.

glucarate was isolated by concentration to dryness, addition of the minimum volume of H_2O necessary to dissolve the sample, titration to pH 11 with 45% KOH to ensure delactonization, and careful addition of HCl to pH ~4, after which the monopotassium salt of glucarate crystallized from solution in small white needles (0.912 g, 3.66 mmol, mp 189 °C): ^{1}H NMR δ (D_2O) 4.16 (d, $J = 3.1$ Hz, H-2), 4.10 (dd, $J = 4.4$, 4.7 Hz, H-5), 3.96 (dd, $J = 3.1$, 5.3 Hz, H-3), 3.81 (ddd, $J = 3.6$, 4.7, 5.3 Hz, H-4); ^{13}C δ (H_2O) 178.2. The (*L*)-[1(6)-^{13}C]Idarate was isolated in a similar fashion, except precipitation at pH 4 was effected by addition of 2-propanol. The resulting solid was recrystallized from H_2O−2-propanol, yielding small white needles (0.344 g, 1.38 mmol, mp 170 °C): ^{1}H NMR δ (D_2O) 4.16 [m, H-2(5)], 3.92 [s, H-3(4)]; ^{13}C NMR δ (H_2O) 178.5. The overall yield of the labeled hexaric acids from (*L*)-xylose was 15%.

Assays of GlucD Activity. The formation of 5-KDG catalyzed by GlucD was performed at 22 °C in 50 mM Tris-HCl, pH (or pD) 8.0, containing 10 mM $MgCl_2$ and quantitated by end point detection of its semicarbazone at 250 nm (*12*).

Kinetic Studies Using ^{1}H and ^{13}C NMR Spectroscopies. Kinetic studies using ^{13}C NMR spectroscopy were performed at 22 °C with 0.1 M substrate [(*D*)-[6-^{13}C]glucarate or (*L*)-[1(6)-^{13}C]idarate] in 50 mM Tris-HCl, pH (or pD) 8.0, containing 10 mM $MgCl_2$, 10% D_2O, and 0.2% dioxane (as internal standard). Kinetic studies using ^{1}H NMR spectroscopy were performed analogously with 0.1 M unlabeled substrates.

RESULTS AND DISCUSSION

Reactions Catalyzed by GlucD. We recently reported that GlucD from *P. putida* catalyzes the dehydration of both (*D*)-glucarate and (*L*)-idarate to a single product, 5-KDG, as well as catalyzing the epimerization of (*D*)-glucarate and (*L*)-idarate (*6*). These conclusions contradicted the earlier report that GlucD catalyzes two regiodistinct dehydrations of (*D*)-glucarate (*2*).

The values for the kinetic constants using both (*D*)-glucarate and (*L*)-idarate are summarized in Table 1.[3] While the value for k_{cat} for the dehydration of (*L*)-idarate exceeds

[3] The previously reported values of k_{cat} for dehydration of both (*D*)-glucarate and (*L*)-idarate, 3 s^{-1} and 4 s^{-1}, respectively (*6*), are incorrect due to an arithmetic error.

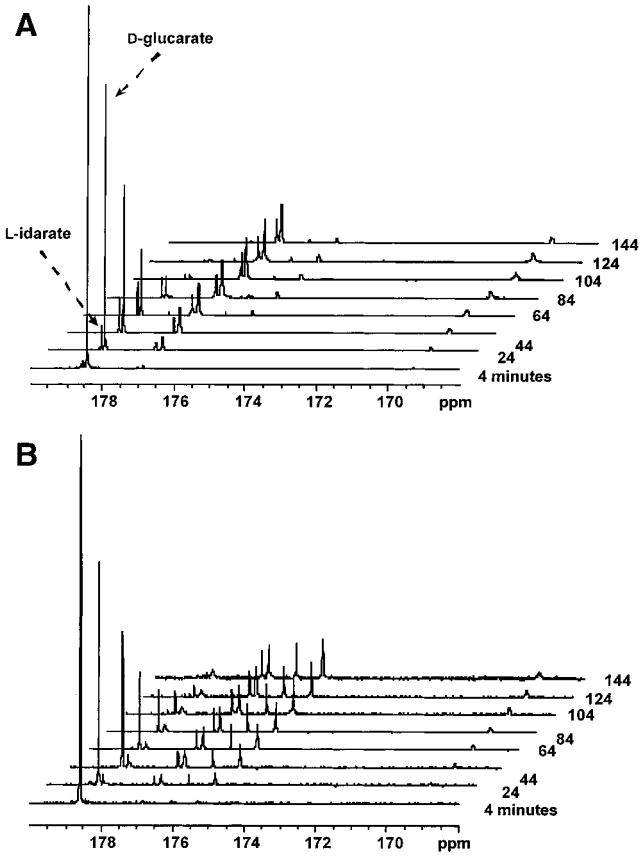

FIGURE 1: Panel A: Partial ^{13}C NMR spectra of the reaction of (*D*)-[6-^{13}C]glucarate in the presence of GlucD at pH 8.0. Panel B: Partial ^{13}C NMR spectra of the reaction of (*L*)-[1(6)-^{13}C]idarate in the presence of GlucD at pH 8.0. The assignments of the resonances are detailed in the text.

that for (*D*)-glucarate, (*D*)-glucarate is a "better" substrate as assessed by the values of k_{cat}/K_m.

^{13}C NMR Studies. The multiple reactions catalyzed by GlucD (*6*) were confirmed and quantitated by monitoring the ^{13}C NMR spectra of reaction mixtures containing either (*D*)-[6-^{13}C]glucarate or (*L*)-[6-^{13}C]idarate.

Spectra depicting the time course of a reaction using (*D*)-[6-^{13}C]glucarate as substrate are shown in Figure 1, panel A. In concert with disappearance of the resonance associated with carbon-6 of the substrate (178.2 ppm), resonances appear that are associated with carbon-6 of the keto form (near 168 ppm) as well as α- and β-anomers of the hemiketal form (Scheme 2; near 177 ppm) of the [6-^{13}C]-5-KDG product. Importantly, a signal associated with (*L*)-[1(6)-^{13}C]-idarate (178.5 ppm) also appears that increases to a maximum and then decreases as it also is dehydrated to 5-KDG.

Because (*L*)-idarate is symmetrical, the ^{13}C-label that originated in carbon-6 of (*D*)-glucarate is "scrambled" into both the carbon-1 and carbon-6 positions of (*L*)-idarate. As the (*L*)-[1,6-^{13}C]idarate is dehydrated, resonances associated with carbons-1 of the α- and β-anomers of the hemiketal of 5-KDG appear near 176 and 175 ppm. In the spectra shown in Figure 1, the resonance associated with the keto form of [1-^{13}C]-5-KDG expected at 178.1 ppm is not visible since this species has not accumulated sufficiently.

Spectra depicting the time course of a reaction using (*L*)-[1(6)-^{13}C]idarate as substrate are shown in Figure 1, panel B. As the resonance associated with the substrate decreases

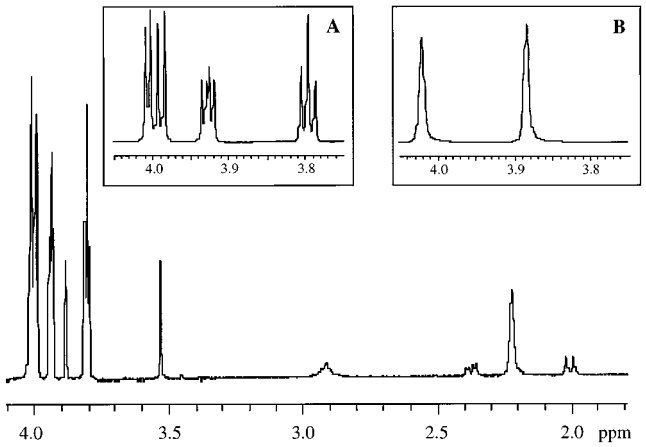

FIGURE 2: Partial ^{1}H NMR spectrum of (*D*)-glucarate in the presence of GlucD at pH 8.0 after ~33% reaction. Inset A: Spectrum of (*D*)-glucarate in the absence of enzyme. Inset B: Spectrum of (*L*)-idarate in the absence of enzyme.

(178.5 ppm), resonances appear that are associated with the keto and hemiketal forms of 5-KDG labeled equivalently at carbons-1 and -6. The resonance associated with (*D*)-[6-^{13}C]glucarate appears and increases with time before being converted to the 5-KDG product. The resonance associated with (*D*)-[1-^{13}C]glucarate is obscured by that of the (*L*)-[1,6-^{13}C]idarate substrate. In these spectra, the signal due to the keto form of [1-^{13}C]-5-KDG is visible at 178.1 ppm, partially overlapping that of (*D*)-[6-^{13}C]glucarate at later time points.

^{1}H NMR Studies. The overlap of resonances in the ^{13}C NMR experiments led to the use of ^{1}H NMR for monitoring the progress of the GlucD-catalyzed reactions. Such experiments must be performed in H_2O rather than D_2O to avoid solvent isotope effects on both the rate and product distribution (vide infra); the method used to obtain such spectra is described in the Materials and Methods section.

The partial ^{1}H NMR spectrum of a reaction using (*D*)-glucarate as substrate that had proceeded to about 30% completion is shown in Figure 2. Integration of the intensities of the resolved resonances corresponding to H-3 of (*D*)-glucarate (3.93 ppm), H-3(4) of idarate (3.88 ppm), and H-4 of the keto and hemiketal forms of 5-KDG (2.91, 2.37, 2.21, and 2.01 ppm) relative to the internal dioxane standard (3.53 ppm) allows the amounts of (remaining) substrate, intermediate [(*L*)-idarate], and product (5-KDG) to be quantitated. The complete time course of the reaction is shown in Figure 3.

From these data, we conclude that the presumed enolic intermediate (Scheme 2) is partitioned between dehydration and epimerization in a 4:1 ratio, revealing that the k_{cat} for epimerization of (*D*)-glucarate is ~4 s^{-1} (25% of the measured k_{cat} for dehydration). Since the production of 5-KDG is linear with time and does not lag behind the transient accumulation of (*L*)-idarate, the dehydration of (*D*)-glucarate does not require the formation of (*L*)-idarate as an essential intermediate. Since GlucD presumably has evolved for the purpose of catabolizing (*D*)-glucarate and not the unnatural (*L*)-idarate to 5-KDG, that dehydration is favored over epimerization is not surprising.

The results of analogous ^{1}H NMR experiments using (*L*)-idarate as substrate are summarized in Figure 4. In this case, the initial rate of formation of the dehydration product

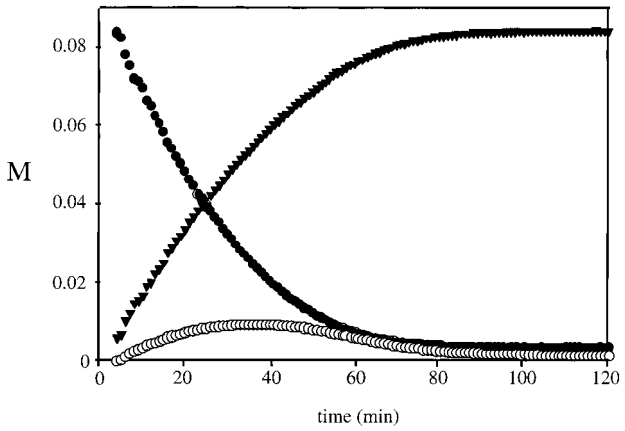

FIGURE 3: Time course of the reaction of (*D*)-glucarate in the presence of GlucD at pH 8.0: ● = (*D*)-glucarate; ○ = (*L*)-idarate; ▼ = 5-KDG. Concentrations were determined on the basis of integration of the ^{1}H NMR spectra recorded at 1 min intervals.

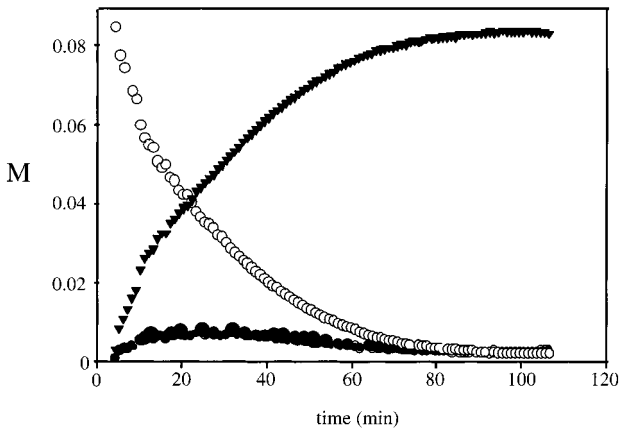

FIGURE 4: Time course of the reaction of (*L*)-idarate in the presence of GlucD at pH 8.0: ○ = (*L*)-idarate; ● = (*D*)-glucarate; ▼ = 5-KDG. Concentrations were determined on the basis of integration of the ^{1}H NMR spectra recorded at 1 min intervals.

5-KDG exceeds that of epimerization by a 3:1 ratio, revealing that the k_{cat} for epimerization of (*L*)-idarate is ~7 s^{-1} (33% of the measured k_{cat} for dehydration). The production of 5-KDG also is linear with time, so the dehydration of (*L*)-idarate also does not require the formation of (*D*)-glucarate as an essential intermediate.

Substrate Deuterium Kinetic Isotope Effects. The substrate deuterium kinetic isotope effects (KIEs) were measured using (*D*)-[2,3,4,5-$^2H_4$]glucarate and (*L*)-[2,5-$^2H_2$]idarate. Perdeuterated (*D*)-glucarate was more conveniently obtained [from commercially available perdeuterated (*D*)-glucose] than either (*D*)-[5-^{2}H]glucarate or (*D*)-[2,5-$^2H_2$]glucarate [a side product of the preparation of (*L*)-[2,5-$^2H_2$]idarate from 5-ketofructose (vide supra)]. The presence of deuterons at carbons-2, -3, and -4 is not expected to have a large effect, although a small (≤20%) secondary KIE from deuteration at carbon-4 is possible.

The formation of 5-KDG from both (*D*)-glucarate and (*L*)-idarate is subject to a substrate deuterium KIE on k_{cat} (Table 1); the value for (*D*)-glucarate is 4.1, and that for (*L*)-idarate is 2.6. Considering the possible number of steps that contribute to k_{cat}, these values suggest that the transition states for proton abstraction from carbons-5 of both (*D*)-glucarate and (*L*)-idarate play a dominant role in determining k_{cat}. This finding is not unexpected, considering the energetic barrier

associated with abstraction of a proton from the carbon adjacent to a carboxylate group; i.e., the pK_a of the 5-proton of either (*D*)-glucarate or (*L*)-idarate is expected to be ~32 (*13*).

Solvent Deuterium Kinetic Isotope Effects. With (*D*)-glucarate as substrate, the solvent deuterium KIE on k_{cat} for the formation of 5-KDG is 2.1. When (*L*)-idarate is the substrate, the value of the solvent deuterium KIE is 3.0. Multiple hydrogen-bonding interactions are present in the enzyme−substrate, −transition state, −intermediate, and −product complexes which would be affected by the change in solvent isotope, so it can be erroneous to attribute the observed KIEs to a simple effect on a single proton transfer reaction (*14*).

A solvent KIE of similar magnitude was observed in the racemization of (*S*)-mandelate catalyzed by the K166R mutant of MR, a process in which enolization is thought to be the rate-determining step (*15*). The measured values of the solvent KIEs in the GlucD-catalyzed reactions are in accord with the magnitude expected for the partial transfer of a proton from a general acidic catalyst in the formation of an intermediate stabilized by enhanced hydrogen-bonding interactions (*16*). In support of this interpretation, the values of the substrate deuterium KIEs on k_{cat} are consistent with formation of a stabilized enolic intermediate contributing significantly to the rate-determining step with both substrates.

Alternatively, the value of the solvent KIE could be used as evidence of rate-determining Brønsted acid-catalyzed departure of the leaving hydroxyl group; however, given the value of the substrate KIE, this interpretation is unlikely. In fact, departure of the leaving hydroxyl group might be assisted by a Lewis acid, i.e., an active site Mg^{2+}.[4]

We previously described that the reaction of ^{13}C-labeled (*D*)-glucarate with GlucD is accompanied by scrambling of the label in the dehydration product due to intermediate formation of symmetrical (*L*)-idarate (*6*). In unpublished experiments, we observed that this scrambling was markedly reduced [from about 15% to about 2% as assessed by integration of ^{1}H and ^{13}C NMR spectra of the labeled (*L*)-idarate product] when the reactions were performed in buffers prepared with D_2O rather than with H_2O. We interpret this decrease in scrambling as the result of the primary solvent KIE on protonation of the enolic intermediate (Scheme 2) that generates [2(5)-^{2}H$_1$,1(6)-^{13}C]-(*L*)-idarate. A decrease in the rate of this step would reduce the steady-state concentration of the (*L*)-idarate that is formed in competition with dehydration and, therefore, the amount of isotopic scrambling.

Free Energy Profile for the GlucD-Catalyzed Reactions. The free energy profile shown in Figure 5 describes the relative energies of bound (*D*)-glucarate, (*L*)-idarate, and the enolic intermediate (Scheme 2). The relative energies were determined by the measured values for k_{cat} for dehydration and epimerization of both (*D*)-glucarate and (*L*)-idarate, the substrate KIEs on k_{cat} for both (*D*)-glucarate and (*L*)-idarate, and the observation that solvent deuterium markedly decreases the amount of isotopic scrambling.

[4] Activity measurements and EPR studies using Mn^{2+} indicate that GlucD binds and is dependent on two divalent metal ions for activity (*28*).

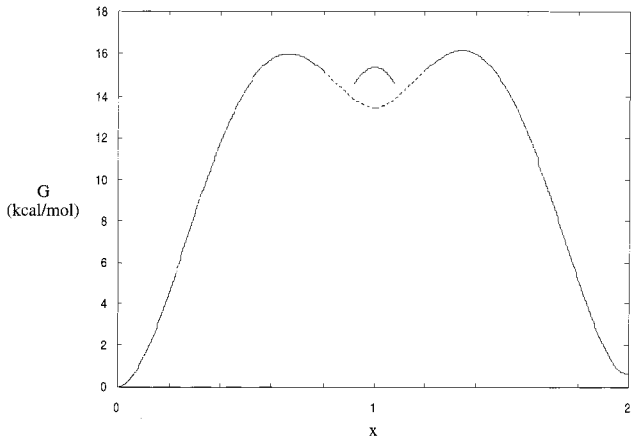

FIGURE 5: Proposed dependence of *G* on the position of the reaction coordinate, *x*, for the GlucD-catalyzed epimerization of (*D*)-glucarate and (*L*)-idarate and the vinylogous β-elimination reaction to yield 5-KDG. (*D*)-Glucarate bound in the active site is at $x = 0$, the enolic intermediate (Scheme 2) that partitions between epimerization and β-elimination is at $x = 1$, and (*L*)-idarate is at $x = 2$. The energy of the enolic intermediate is unknown and is shown by the dotted line in the diagram; the transition state for vinylogous β-elimination is represented by the solid parabola above this dotted line. The reaction coordinate is drawn to illustrate a difference of 0.6 kcal/mol in the energies of bound (*D*)-glucarate and (*L*)-idarate (describing the differences in the values of their K_ms), a difference of 0.15 kcal/mol between the transition states for abstraction of the α-protons from (*D*)-glucarate and (*L*)-idarate, and a difference of 0.7 kcal/mol between the transition states for abstraction of the α-proton from (*D*)-glucarate and the vinylogous β-elimination reaction that yields 5-KDG. The latter energies are calculated from the observed partitioning of the enolic intermediate between epimerization and β-elimination. The absolute energies are calculated on the basis of transition state theory and the measured k_{cat}s for the various reactions.

For both substrates we conclude that the transition states leading to formation of the stabilized enolic intermediate predominate in determining k_{cat}, as judged by the large values of the substrate KIEs and the pronounced effect of solvent deuterium on the partitioning of the enolic intermediate between dehydration and epimerization. The small differences in the values for the k_{cat}s for dehydration of both (*D*)-glucarate and (*L*)-idarate reflect the similar energies of the transition states for abstraction of the α-proton to generate what is expected to be a chemically identical enolic intermediate (Scheme 2). The small differences in the measured ratios for partitioning the common enolic intermediate between dehydration and epimerization confirm this conclusion and reveal that the transition state for the vinylogous β-elimination of water from the enolic intermediate to generate a second intermediate (the enol intermediate in Scheme 2) is only slightly lower in energy (by ~0.7 kcal/mol) than those for the 1,1-proton transfer reactions that lead to epimerization.

This latter small difference in free energy is consistent with the proposals put forth by Albery and Knowles regarding the evolution of enzyme activities (*17*): no selection can be expected for decreasing the free energy of the transition state for dehydration if the free energy of the transition state for the preceding abstraction of the α-proton is greater. Only by decreasing the free energy of the transition state for abstraction of the α-proton can the free energy of the subsequent transition state for dehydration be decreased.

These features of the free energy diagram for the GlucD-catalyzed reaction can be compared with those deduced for the mandelate racemase-catalyzed reaction (*18*). In the MR-catalyzed reaction, the available evidence supports the intermediacy of a common stabilized enolic intermediate, although the concentration of the intermediate has not been quantitated. In this reaction, the transition states for formation of the intermediate from the substrate enantiomers also are thought to be nearly isoenergetic.

In both the MR- and GlucD-catalyzed reactions, abstraction of the α-proton from the enantiomeric/epimeric substrates is accomplished by different functional groups, presumably a lysine-derived amino group from (*S*)-mandelate/(*D*)-glucarate (Lys 164 and Lys 213, respectively) and a histidine-derived imidazole group from (*R*)-mandelate/(*L*)-idarate (His 270 and His 345, respectively). That the transition states are nearly equivalent in free energy in both reactions reflects a modulation of their inherent relative reactivities by the active site environment, e.g., a possible reduction in the pK_a of the conjugate acid of the lysine by electrostatic effects. The structural origin of this effect is not yet understood.

Stereochemistry of Tautomerization. β-Elimination of water from carbons-5 and -4 presumably from either (*D*)-glucarate or (*L*)-idarate yields what is also expected to be a chemically identical and transiently stable enol intermediate that tautomerizes to form the observed 5-KDG product (Scheme 2). We recently reported (*19*) that when the reaction is performed in D_2O, tautomerization of this intermediate is accompanied by incorporation of a solvent-derived deuterium at carbon-4. Irrespective of whether the substrate is (*D*)-glucarate or (*L*)-idarate, the deuteron is incorporated stereospecifically in the *pro-S* position. This is evidence that the tautomerization step occurs within the chiral environment of the enzyme active site. That a single monodeuterated product is formed regardless of the configuration of the substrate supports our hypothesis that both substrates generate the same enol intermediate, as shown in Scheme 2.

Evolution of the Enolase Superfamily. We (*4*, *20*) have noted that enzymes that catalyze diverse overall reactions can be homologous. The MR group of the enolase superfamily contains enzymes that catalyze only racemization reactions (MR) as well as only dehydration (β-elimination) reactions [(*D*)-galactonate dehydratase from *E. coli*; refs *19*, and *21*]. If these enzymes have evolved from a common progenitor, then gratifying evidence would be provided by an enzyme that catalyzes both activities *with its natural substrate*, particularly if one of these reactions were of no apparent benefit to the organism. GlucD is just such an enzyme, providing a "missing link" between the enzymes that catalyze β-elimination reactions and those that catalyze racemization reactions. The formation of (*L*)-idarate from (*D*)-glucarate is metabolically cryptic, although clearly it is not toxic. We have confirmed that *E. coli* can utilize (*L*)-idarate as the sole carbon source, with no apparent reduction in growth rate relative to growth on (*D*)-glucarate. To the best of our knowledge, (*L*)-idarate is not found in nature, so no apparent metabolic pressure exists for utilizing (*L*)-idarate as the carbon source. (*L*)-Iduronic acid residues are found in molecules such as heparin, and a nonspecific oxidase enzyme could form (*L*)-idarate from (*L*)-iduronate *in simile* with (*D*)-glucarate formation. However, all known iduronyl species are formed by C-5 epimerization of the corresponding (*D*)-glucuronyl compound (*22*), making epimerization of (*D*)-glucarate and (*L*)-idarate metabolically unnecessary.

Our premise is that studying the members of a superfamily of enzymes in concert allows more mechanistic information about each enzyme to be gained than would be possible by studying the enzymes individually. This advantage is clearly illustrated by our investigation of the mechanism of the GlucD-catalyzed reaction: in the absence of primary sequence alignments, along with our understanding of the reactions catalyzed by enolase, MR, MLE, and GalD, the epimerization reaction catalyzed by GlucD would not have been recognized, much less predicted. Furthermore, tautomerization of the enol "product" of the β-elimination reaction to the ketone product would not necessarily have been expected to be catalyzed within the active site of GlucD in the absence of a predictive model. However, when such enzyme-catalyzed tautomerization was observed for the analogous dehydration reaction catalyzed by the homologous (*D*)-galactonate dehydratase, we predicted and subsequently confirmed that this would be the case for the GlucD-catalyzed reaction (*19*).

On the basis of the available crystal structures of members of the enolase superfamily, namely, MR (*23*, *24*), MLE (*25*; M. Hasson, I. Schlicting, J. Moulai, D. Ringe, and G. Petsko, unpublished observations), and enolase (*26*, *27*), we would expect the structure of GlucD to be composed of a β-barrel domain with an N-terminal domain containing a flexible loop that closes over the active site during the reaction. Crystallographic studies reported in an accompanying paper indicate that this is, in fact, the case (*7*).

ACKNOWLEDGMENT

The authors thank Dr. Patricia C. Babbitt, University of California at San Francisco, for helpful discussions and the VOICE-NMR Laboratory in the School of Chemical Sciences at the University of Illinois for technical assistance.

REFERENCES

1. Blumenthal, H. J. (1966) *Methods Enzymol. 9*, 660−665.
2. Jeffcoat, R., Hassall, H., and Dagley, S. (1969) *Biochem. J. 115*, 969−976.
3. Ogawa, K., Akagawa, E., Nakamura, K., and Yamane, K. (1995) *Microbiology 141*, 269−275.
4. Hubbard, B. K., Koch, M., Palmer, D. R. J., Babbitt, P. C., and Gerlt, J. A. (1998) *Biochemistry 37*, 14369−14375.
5. Babbitt, P. C., Hasson, M. S., Wedekind, J. E., Palmer, D. R. J., Barrett, W. C., Rayment, I., Ringe, D., Kenyon, G. L., and Gerlt, J. A. (1996) *Biochemistry 35*, 16489−16501.
6. Palmer, D. R. J., and Gerlt, J. A. (1996) *J. Am. Chem. Soc. 118*, 10323−10324.
7. Gulick, A. M., Palmer, D. R. J., Babbitt, P. C., Gerlt, J. A., and Rayment, I., (1998) *Biochemistry 37*, 14358−14368.
8. Abdel-Akher, M., Hamilton, J. K., and Smith, F. (1951) *J. Am. Chem. Soc. 73*, 4691−4692.
9. Mehltretter, C. L. (1961) *Methods Carbohydr. Chem. 2*, 46−48.
10. Avigad, G., and Englard, S. (1975) *Methods Enzymol. 41*, 84−90.

11. Serianni, A. S., Nunez, H., and Barker, R. (1980) *J. Org. Chem. 45*, 3329−3341.
12. MacGee, J., and Doudoroff, M. (1954) *J. Biol. Chem. 210*, 617−624.
13. Gerlt, J. A., Kozarich, J. W., Kenyon, G. L., and Gassman, P. G. (1991) *J. Am. Chem. Soc. 113*, 9667−9669.
14. Kresge, A. J. (1973) *J. Am. Chem. Soc. 95*, 3065−3067.
15. Kallarakal, A. T., Kozarich, J. W., Gerlt, J. A., Clifton, J. R., Petsko, G. A., and Kenyon, G. L. (1995) *Biochemistry 34*, 2788−2797.
16. Gerlt, J. A., and Gassman, P. G. (1993) *J. Am. Chem. Soc. 115*, 11552−11568.
17. Albery, W. J., and Knowles, J. R. (1976) *Biochemistry 15*, 5631−5640.
18. Mitra, B., Kallarakal, A. T., Kozarich, J. W., Gerlt, J. A., Clifton, J. R., Petsko, G. A., and Kenyon, G. L. (1995) *Biochemistry 34*, 2777−2787.
19. Palmer, D. R. J., Wieczorek, S. J., Hubbard, B. K., Mrachko, G. T., and Gerlt, J. A. (1997) *J. Am. Chem. Soc. 119*, 9580−9581.
20. Babbitt, P. C., and Gerlt, J. A. (1997) *J. Biol. Chem. 272*, 30591−30594.
21. Babbitt, P. C., Mrachko, G. T., Hasson, M. S., Huisman, G. W., Kolter, R., Ringe, D., Petsko, G. A., Kenyon, G. L., and Gerlt, J. A. (1995) *Science 267*, 1159−1162.
22. Hannesson, H. H., Magner-McWhirter, A., Tiedemann, K., Lindahl, U., and Malmstrom, A. (1996) *Biochem. J. 313*, 489−596.
23. Neidhart, D. J., Howell, P. L., Petsko, G. A., Powers, V. M., Li, R. S., Kenyon, G. L., and Gerlt, J. A. (1991) *Biochemistry 30*, 9264−9273.
24. Landro, J. A., Gerlt, J. A., Kozarich, J. W., Koo, C. W., Shah, V. J., Kenyon, G. L., Neidhart, D. J., Fujita, S., and Petsko, G. A. (1994) *Biochemistry 33*, 635−643.
25. Helin, S., Kahn, P. C., Guha, B. L., Mallows, D. G., and Goldman, A. (1995) *J. Mol. Biol. 254*, 918−941.
26. Wedekind, J. E., Poyner, R. R., Reed, G. H., and Rayment, I. (1994) *Biochemistry 33*, 9333−9342.
27. Larsen, T. M., Wedekind, J. E., Rayment, I., and Reed, G. H. (1996) *Biochemistry 35*, 4349−4358.
28. Budihas, S. R. (1997) Ph.D. Thesis, University of Illinois.

BI981122V